Extensive features of tight oligosaccharide binding revealed in high-resolution structures of the maltodextrin transport/chemosensory receptor

Florante A Quiocho[1,2]*, John C Spurlino[1†] and Lynn E Rodseth[3]

Background: Active-transport processes perform a vital function in the life of a cell, maintaining cell homeostasis and allowing access of nutrients. Maltodextrin/maltose-binding protein (MBP; M_r = 40k) is a receptor protein which serves as an initial high-affinity binding component of the active-transport system of maltooligosaccharides in bacteria. MBP also participates in chemotaxis towards maltooligosaccharides. The interaction between MBP and specific cytoplasmic membrane proteins initiates either active transport or chemotaxis. In order to gain new understanding of the function of MBP, especially its versatility in binding different linear and cyclic oligosaccharides with similar affinities, we have undertaken high-resolution X-ray analysis of three oligosaccharide-bound structures.

Results: The structures of MBP complexed with maltose, maltotriose and maltotetraose have been refined to high resolutions (1.67 to 1.8 Å). These structures provide details at the atomic level of many features of oligosaccharide binding. The structures reveal differences between buried and surface binding sites and show the importance of hydrogen bonds and van der Waals interactions, especially those resulting from aromatic residue stacking. Insights are provided into the structural plasticity of the protein, the binding affinity and the binding specificity with respect to α/β anomeric preference and oligosaccharide length. In addition, the structures demonstrate the different conformations that can be adopted by the oligosaccharide within the complex.

Conclusions: MBP has a two-domain structure joined by a hinge-bending region which contains the substrate-binding groove. The bound maltooligosaccharides have a ribbon-like structure: the edges of the ribbon are occupied by polar hydroxyl groups and the flat surfaces are composed of nonpolar patches of the sugar ring faces. The polar groups and nonpolar patches are heavily involved in forming hydrogen bonds and van der Waals contacts, respectively, with complimentary residues in the groove. Hinge-bending between the two domains enables the participation of both domains in the binding and sequestering of the oligosaccharides. Changes in the subtle contours of the binding site allow binding of maltodextrins of varying length with similarly high affinities. The fact that the three bound structures are essentially identical ensures productive interaction with the oligomeric membrane proteins, which are distinct for transport and chemotaxis.

Addresses: [1]Howard Hughes Medical Institute, Baylor College of Medicine, Houston, TX 77030, USA, [2]Department of Biochemistry, Baylor College of Medicine, Houston, TX 77030, USA and [3]Department of Biochemistry and Cell Biology, Rice University, Houston, TX 77021, USA.

[†]Present address: 3-Dimensional Pharmaceuticals, Inc. 665 Stockton Dr., Exton, PA 19341, USA.

*Corresponding author.
E-mail: faq@dino.bcm.tmc.edu

Key words: active transport, chemotaxis, maltodextrin-binding protein structure, oligosaccharide conformation, protein–oligosaccharide interactions

Received: 28 April 1997
Revisions requested: 5 June 1997
Revisions received: 27 June 1997
Accepted: 27 June 1997

Structure 15 August 1997, 5:997–1015
http://biomednet.com/elecref/0969212600500997

Introduction

The ability of bacteria, and indeed all cells, to thrive is linked to their ability to utilize specific energy sources. Active-transport systems are an essential factor in the utilization of nutrients. These systems provide an efficient, highly concentrative process of accumulating substances from the surrounding media. Maltodextrin/maltose-binding protein (MBP) is a member of a family of approximately four dozen proteins which serve as initial high-affinity receptors of the ATP-binding cassette (ABC) of active transport systems or permeases in bacteria (for review see [1]). Each active-transport system consists of an initial extracytoplasmic receptor or binding protein and a set of cytoplasmic membrane-associated proteins. The membrane protein complex is the actual facilitator and energy consuming component of transport, but does not function without the binding protein. About four of the periplasmic binding proteins, including MBP, also participate in the simple behavioral response of chemotaxis which requires a different set of membrane protein components [2].

Maltooligosaccharides or maltodextrins represent a commonly available source of energy. The high-affinity transport of oligosaccharides by the MBP-dependent active transport system supplies the bacteria with ample resources to allow rapid growth in minimal media. MBP binds linear maltooligosaccharides or maltodextrins of up to seven α(1–4)-linked glucose (Glc) units [3] which are then transported. In the final step, the maltodextrins are hydrolyzed by enzymes in the cytoplasm (e.g. maltoamylase and maltophosphorylase) to provide shorter maltodextrins and glucose or glucose-1-phosphate for metabolism. The prevalence of amylases and the ease of incorporation of glucose into the metabolic pathway makes maltodextrins a substrate of choice.

The crystal structure of MBP, complexed with maltose, was first determined at 2.3 Å resolution and revealed a two-domain structure [4]. The subsequent report of the 1.8 Å structure of MBP without bound sugar provided the first direct evidence from a member of the family of periplasmic binding proteins for a hinge-bending motion between the two domains [5]. This motion modulates access to and from the ligand-binding site located between the two domains and provides the mechanism critical for signal transduction in both active transport and chemotaxis. The structure of MBP with bound β-cyclodextrin has also been determined at 1.8 Å resolution [6].

In recent years much attention has been directed towards the study of protein–carbohydrate interactions, fuelled by the structure determination of about 40 proteins/enzymes complexed with carbohydrates. Interest in oligosaccharides stems from the diversity of their biological activities and the conformational degrees of freedom they are able to display structurally, as a result of linear and branched chain structure formation. In this paper we describe the high-resolution structure determination of the complexes of MBP with maltose, maltotriose and maltotetraose. The K_d values of these complexes (3.5, 0.16 and 2.3 μM, respectively) reflect some of the tightest protein–carbohydrate interactions. These structures further deepen our understanding, at the atomic level, of the features associated with oligosaccharide recognition and binding. They also provide detailed understanding of the function of the protein.

Results and discussion

The high-resolution structures of the complexes of MBP with linear maltose, maltotriose and maltotetraose (Table 1), together with that of the complex with β-cyclodextrin [6], have enabled us to extensively dissect and solidify understanding of carbohydrate recognition at the atomic level. Many important features of carbohydrate recognition have been elucidated: ligand accessibility and its relationship in formulating two general types or groups of proteins that bind carbohydrates; hydrogen bond interactions; van der Waals interactions arising from aromatic residue stacking; structural plasticity; specificity and affinity; and oligosaccharide conformation. These features, to varying degrees, are encountered in the atomic interactions between other proteins and carbohydrates. Metal-assisted sugar binding, which is seen in only very few protein structures, will not be considered within the scope of this study. Where appropriate, some of the key features of carbohydrate recognition will be further amplified and/or compared with those observed in the equally well refined, high-resolution structures of monosaccharide complexes of the L-arabinose-binding protein (ABP) [7,8], D-glucose/D-galactose-binding protein (GGBP) [9–11], and D-ribose-binding protein (RBP) [12], which are also members of the receptor family.

Our laboratory has also investigated carbohydrate binding to MBP, as well to ABP and GGBP, in solution using equilibrium and rapid-kinetic techniques [13,14] (unpublished results), and the pertinent data are collected in Table 2. The binding affinities of the best ligands to MBP, ABP and GGBP, which do not vary greatly, are some of the tightest among all proteins/enzymes with carbohydrate ligands. MBP can also bind cyclic dextrins (Table 2) [14], although these are nonphysiological substrates as they are not transported across the inner membrane nor do they induce a chemotactic response [15].

The K_d values, which compare well with k_{-1}/k_1 ratios, show no enormous systematic enhancement in affinity with increasing length of the linear oligosaccharides or with the more rigid cyclic dextrins. In fact the best ligand is maltotriose, exhibiting a K_d that is tenfold to 30-fold lower than those of the other ligands. In contrast to the variation of the K_ds, the bimolecular kinetic rate constant k_1 values remain nearly constant for all oligosaccharides tested. The changes in the K_d values correlate well with changes in the k_{-1} values. Variations in the k_{-1} values reflect the stability provided by the ligand on complex formation.

Refined structures

Structures

The structures with bound maltose, maltotriose, and maltotetraose were refined to crystallographic R factors of 0.182 (to 1.67 Å resolution), 0.164 (to 1.7 Å resolution) and 0.194 (to 1.8 Å resolution), respectively (Table 1). Initial coordinates for the refinements were obtained from the structure of the MBP–maltose complex refined at 1.7 Å resolution [16] (see Materials and methods section). The geometry of all three structures is good and well within accepted limits. As the binding-site region, together with the bound oligosaccharide, exhibits B factors about two times lower than the average B factor of the entire protein model (26.8–30.8 Å^2), this region is more ordered. An electron-density map in the region of the

Table 1

MBP structure refinement statistics.

Parameter	Oligosaccharide			Target
	Maltose	Maltotriose	Maltotetraose	
Resolution range (Å)	10–1.67	10–1.70	10–1.80	
R factor	0.182	0.164	0.194	
Average F_o–F_c	51.41	44.77	19.93	
No. unique reflections	34 825	29 814	27 946	
No. of nonhydrogen atoms	3002	3017	3024	
protein	2875	2875	2875	
sugar	23	34	45	
solvent	104	112	108	
Rms deviation				
bond distances (Å)	0.026	0.027	0.019	0.020
angle distances (Å)	0.055	0.053	0.035	0.030
planar 1–4 distances (Å)	0.078	0.065	0.049	0.050
planarity (Å)	0.014	0.014	0.012	0.015
chiral volume (Å^3)	0.160	0.154	0.202	0.100

bound maltotriose is shown in Figure 1. The root mean square (rms) differences of superimposed Cα atom positions (Figure 2) between MBP–maltose and MBP–maltotriose, MBP–maltose and MBP–maltotetraose, and MBP–maltotriose and MBP–maltotetraose are 0.43, 0.44 and 0.25 Å, respectively.

The MBP structure resembles those of a dozen other binding protein receptors with specificities for carbohydrates, amino acids, oxyanions, oligopeptides, and polyamine with mass ranging from 26–58 kDa [17–19]. The structure is ellipsoidal in shape (axial ratio of 2:1) and composed of two globular domains separated by a deep groove which contains the oligosaccharide-binding site. (For uniformity among binding protein structures, the domains are identified as I and II, which correspond to the previous identifications of N and C domains, respectively [4,7,20].) Each domain of MBP is folded from two segments of the N- and C-terminal halves of the polypeptide chain which result in the formation of three short segments or hinges connecting the two domains (Figure 2). Nevertheless, both domains exhibit similar

Table 2

Equilibrium and rapid kinetics of carbohydrate binding to periplasmic receptors.

Receptor*	Carbohydrate binding †				
	Saccharide	$K_d \times 10^7$ (M)	$k_1 \times 10^{-7}$ (M^{-1} s^{-1})	k_{-1} (s^{-1})	$k_{-1}/k_1 \times 10^7$ (M)
MBP	Maltose	35	2.3	90	39.1
	Maltotriose	1.6	2.5	8.4	3.4
	Maltotetraose	23	2.4	90	39.1
	Maltopentaose	50	2.9	172	59.3
	Maltohexaose	34	2.4	142	59.2
	Maltoheptaose	16	2.3	65	28.4
	α-Cyclodextrin (cyclic maltohexaose)	40	3.6	110	30.6
	β-Cyclodextrin (cyclic maltoheptaose)	18	2.2	46	20.9
ABP	L-Arabinose	0.98	2.4	1.5	0.6
	D-Galactose	2.3	0.8	1.8	2.3
	D-Fucose	38.0	1.2	37.0	30.8
GGBP	D-Galactose	4	3.3	3.4	1.0
	D-Glucose	2	3.5	1.4	0.4

*MBP, maltodextrin-binding protein; ABP, L-arabinose-binding protein; GGBP, D-glucose/D-galactose-binding protein. †K_d is the dissociation constant obtained by equilibrium binding measurements. The bimolecular kinetic rate constants k_1, or association rate, and k_{-1}, or dissociation rate, were obtained by using the rapid-mixing, stopped-flow technique [13,14] (unpublished results).

Figure 1

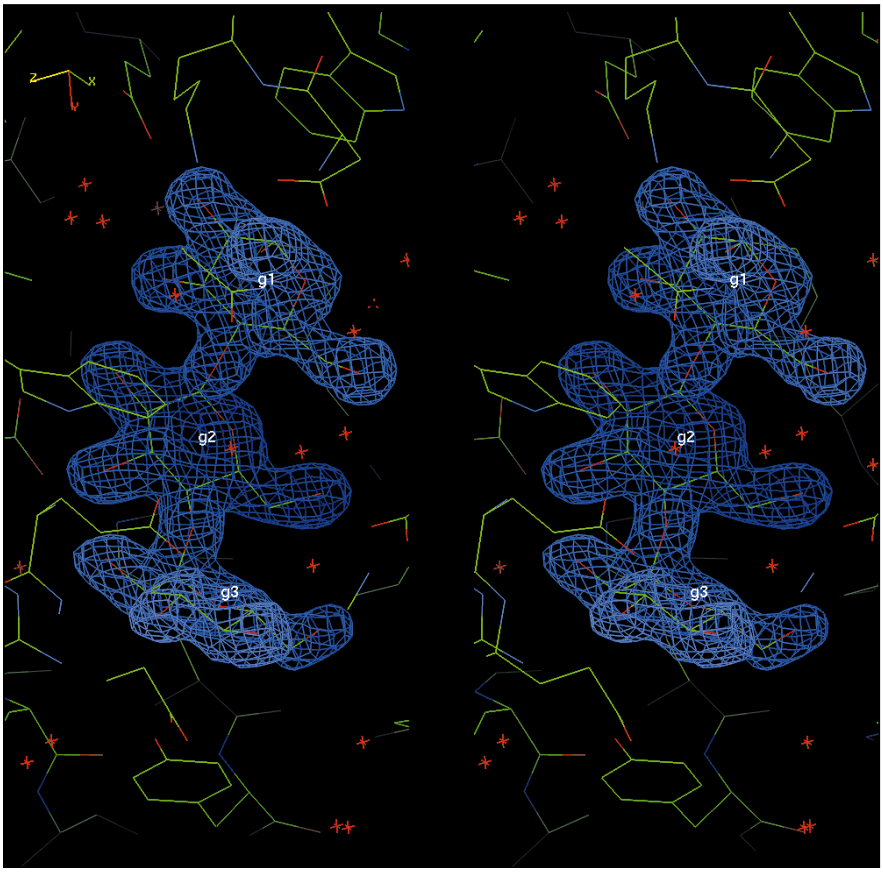

Stereo view of the electron density centered at the maltotriose bound to the maltodextrin-binding protein. The map was calculated with (F_o–F_c, α_c) to 1.7 Å resolution, omitting the maltotriose coordinates, and contoured at 2σ level. The glucosyl (Glc) units are labeled: g1, g2 and g3.

packing of the secondary structure elements; they are composed of a core of β sheet flanked on both sides by helices (Figure 2). Domain II also has a subdomain which extends the sugar-binding groove [4].

Subsites

All of the Glc units common to any pair of the three different bound oligosaccharides superimpose well and occupy identical subsites (Figure 2). For convenience and ease of

Figure 2

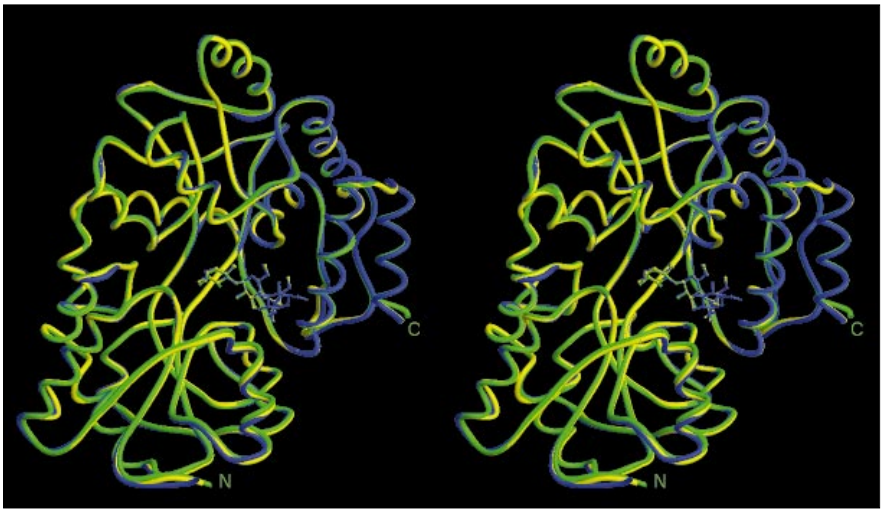

Stereo view of the Cα backbone traces of the maltodextrin-binding protein with bound maltose (green), maltotriose (yellow) and maltotetraose (blue). N and C labels identify the N- and C-terminal ends, respectively; the bound oligosaccharide is shown in stick representation. Domains I and II are on the bottom and top, respectively.

presentation, we continue to use the nomenclature initially formulated to describe the binding of maltose to these subsites [4]. The Glc residues are identified as g1, g2, g3 and g4 moving in the direction from the reducing to the non-reducing end of the sugar, and the subsites within which each corresponding Glc unit resides are identified as S1, S2, S3 and S4, respectively. As the oligosaccharide-binding groove encompasses both domains, the full complements of the subsites are formed only after the two domains come close together by way of a bending motion of a hinge between the two domains [4,5].

Maltodextrins and complementarity

The complementarity between the binding site and the oligosaccharides is extensive and illustrative of tight binding. Carbohydrates, especially the pyranosides, contain a mixture of polar and nonpolar groups of atoms. The linear maltodextrins adopt a ribbon-like shape with a left-handed curvature. Whereas the hydrophobic CH groups are concentrated on the outside and inside surfaces of the ribbon structure, the hydroxyl groups are confined to both edges of the ribbon. Furthermore, the distribution of each atom group is asymmetric. The outside surface contains more hydrophobic patches of CH groups than the inside surface. One edge is populated by two hydroxyl groups (O2 and O3), and the opposite edge is occupied by only one hydroxyl group (O6). These asymmetric distributions are also reflected in oligosaccharide binding to MBP; more aromatic residues, mostly located in domain II, interface with the outside curve of the ribbon than the inside curve, and more hydrogen-bonding residues, mostly in domain I, are directed to the edge lined by two hydroxyl groups than to that lined by one hydroxyl group.

Accessibility of bound oligosaccharides and two general classes of proteins that bind carbohydrates

As first seen in the MBP structures [4,5], access to and from the binding cleft of the periplasmic binding proteins is modulated by the bending of a hinge between the two domains. This conformational change allows the two domains to bind and sequester the ligand. The solvent-accessible surface of individual Glc residues is a good measure of the extent to which each unit is buried. In calculating the solvent accessibility of each Glc, the glycosidic bond oxygen is associated with g2, g3 or g4. The relative accessible surface was calculated by dividing the accessible surface of the bound sugar in the structure (without surface water molecules) by the accessible surface of the unbound sugar in the same conformation.

The bound oligosaccharides are mostly buried. Of the total accessible surfaces of the unbound maltose (157 Å^2), maltotriose (206 Å^2) and maltotetraose (275 Å^2), only 5.2 Å^2, 10.5 Å^2 and 69.4 Å^2, respectively, are not shielded upon binding to MBP. The g2 residue is the least solvent accessible, amounting to 0.9, 0.2 and 0.4% of the accessible surface of the bound maltose, maltotriose, and maltotetraose, respectively. The larger solvent-exposed area of maltotetraose is mainly due to g4 being located halfway out of the groove. As the OH6 of g1 makes two hydrogen bonds with two water molecules close to the surface, it is the most exposed moiety of this Glc unit.

We have divided, or classified, all proteins/enzymes that bind carbohydrates into two broad groups primarily on the basis of the location of the binding sites [21,22]. The sites in proteins belonging to group I (e.g. hexokinase, periplasmic monosaccharide-binding proteins, the phosphorylase active site, members of the LacI family of repressors, etc.) are buried and able to sequester carbohydrates, whereas those of group II (e.g. phosphorylase storage site, lectins, immunoglobulins, amylases) are on or near the protein surface. It is noteworthy that most of the members of group II are multivalent. The affinity of group I proteins for carbohydrates is generally higher than that of group II proteins.

As the Glc units bound in S1, S2 and S3 are buried and the g4 of the maltotetraose in S4 is half exposed on the surface, the binding site groove of MBP exhibits features of the two protein groups. These features are, however, dominated by those of group I. In contrast ABP, GGBP and RBP strictly belong to group I. Features of the binding sites that distinguish the two protein groups will be further underscored below as they are reflected in the structures of MBP.

A characteristic of group I proteins is the significantly lower isotropic averaged temperature factor of the bound sugar and binding site residues relative to that of the entire protein structure. For group II proteins, the difference is often not too great. For example, the averaged B factors of the bound maltose and maltotriose are 17.2 Å^2 and 14.4 Å^2, respectively. The higher averaged B factor of 24.1 Å^2 for the bound maltotetraose is largely due to a much greater B factor of the g4 atoms.

Many of the proteins/enzymes of group I contain two domains which engulf the bound sugars. However, cellobiohydrolase I and maltoporin also belong to group I, but their binding sites are located in a tunnel and a pore, respectively [23,24].

Hydrogen bonds

As hydroxyl groups constitute the major exposed peripheral polar groups of sugars, it is not surprising to find hydrogen bonds, by way of these groups, as a prominent feature of molecular recognition and binding by proteins. This feature is clearly evident in MBP (Figures 3 and 4; Table 3); the oligosaccharides are held in place by a web of hydrogen bonds. With the exception of the g4 OH4 of maltotetraose which extends out into solution, all hydroxyl groups of the three oligosaccharides are involved in multiple hydrogen bonds; this is often seen in group I protein carbohydrate-

Figure 3

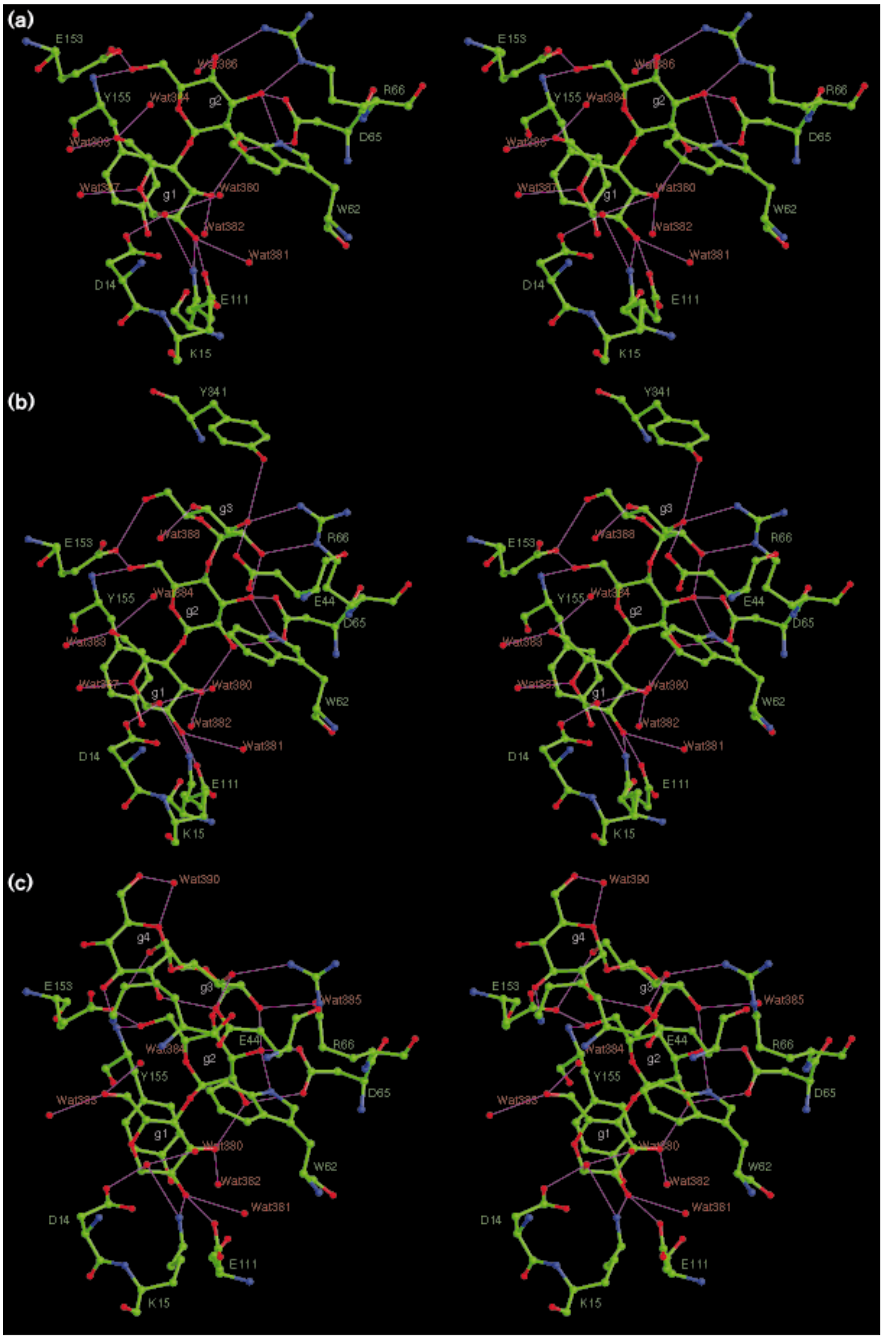

Stereo view of the hydrogen bonds between the maltodextrin-binding protein and maltose (a), maltotriose (b) and maltotetraose (c). Hydrogen bonds are identified with thin lines in magenta, carbon atoms are in green, nitrogen atoms are in blue and oxygen atoms in red.

binding sites. Buried polar groups of the sugar and binding site residues are paired, a stabilizing feature akin to that observed for polar groups inside folded protein structures. The significantly smaller number of hydrogen bonds formed on occupation of S4 by g4 of maltotetraose is characteristic of group II protein carbohydrate-binding sites.

As to be expected, far more hydrogen bonds are associated with the edge of the oligosaccharide ribbon deploying the O2 and O3 hydroxyl groups than with the opposite edge containing only the O6 hydroxyl group (Figures 3 and 4). Interestingly, this asymmetry is also reflected in the distribution of the hydrogen-bonding residues between the two domains. Of the 13 total residues that make hydrogen bonds with almost all of the O2 and O3 hydroxyls, ten reside in domain I. On the other hand, the only two residues (Glu153 and Tyr153) forming hydrogen bonds with O6 hydroxyl groups originate from domain II. Other

Figure 4

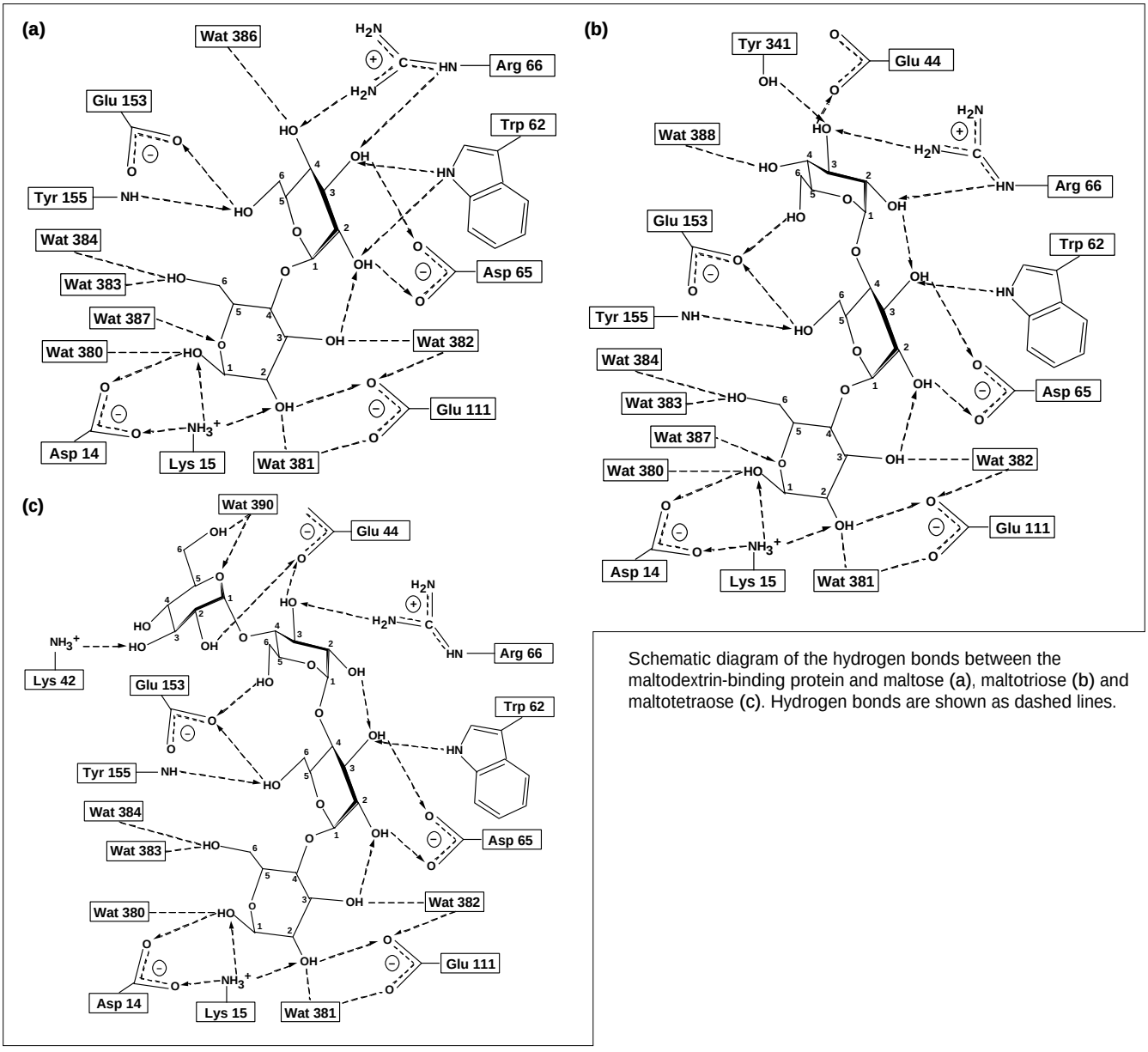

Schematic diagram of the hydrogen bonds between the maltodextrin-binding protein and maltose (a), maltotriose (b) and maltotetraose (c). Hydrogen bonds are shown as dashed lines.

more specific and noteworthy features of the hydrogen-bonding interactions are described as follows using Figures 3 and 4 and Table 3 as references.

Near constant number of hydrogen bonds

Surprisingly, the number of hydrogen bonds associated with maltose, maltotriose and maltotetraose do not vary greatly: 19, 21 and 21, respectively. Direct hydrogen bonds between MBP and oligosaccharides also differ only slightly: 12, 14 and 14 with maltose, maltotriose and maltotetraose, respectively. The difference between the two sets of numbers for a given oligosaccharide represents the number of associated, ordered water molecules. These water molecules, with the exception of 380, 383 and 387 (Table 3), are in turn involved in hydrogen bonds with other residues, thus contributing to the stability of the complexes.

For all the three bound oligosaccharides, g1 and g2 participate in the greatest number of hydrogen bonds, followed by g3. However, g2 makes about twice as many direct hydrogen bonds with MBP as g1. The absence of a constant number of hydrogen bonds to identical Glc residues of the oligosaccharides is attributed to changes in the conformations of the residues involved in binding (further described in Conformational plasticity section

Table 3

Hydrogen bonds to oligosaccharides at the binding site of MBP.

Atom		Distance of ≤ 3.40 Å		
Glc unit	MBP/solvent/sugar	Maltose	Maltotriose	Maltotetraose
g1 O1	Asp14 Oδ2	2.79	2.68	2.62
O1	Lys15 Nζ	3.09	3.19	3.23
O1	Wat380	2.76	2.82	2.85
O2	Lys15 Nζ	2.80	3.00	3.02
O2	Glu111 Oε1	2.65	2.65	2.65
O2	Wat381	2.76	3.13	3.02
O3	Wat382	2.85	2.77	2.72
O5	Wat387	3.04	2.98	
O6	Wat383	2.59	2.91	3.00
O6	Wat384	2.74	2.72	2.94
g2 O2	g1 O3	2.74	2.82	2.66
O2	Asp65 Oδ1	2.71	2.76	2.80
O2	Trp62 Nε1	3.19		
O3	Trp62 Nε1	3.19	2.91	3.07
O3	Asp65 Oδ2	2.84	2.72	2.62
O3	Arg66 Nε	2.75		
O4	Arg66 Nη1	2.77		
O4	Wat386	2.63		
O6	Tyr155 N	3.17	3.16	3.14
O6	Glu153 Oε1	2.51	2.72	2.77
g3 O2	g2 O3		2.75	2.58
O2	Arg66 Nε		2.84	
O3	Glu44 Oε2		2.80	2.62
O3	Arg66 Nη2		2.81	2.82
O3	Tyr341 Oη		3.24	
O4	Wat388		2.42	
O6	Glu153 Oε1		3.20	3.28
g4 O2	g3 O3			(4.00)
O2	Glu44 Oε2			2.79
O3	Lys42 Nζ			2.65
O5	Wat390			3.38
O6	Wat390			3.35
Total*		19	21	21
Protein–sugar only*		12	14	14

*A summary of the number of hydrogen bonds, excluding those between Glc units.

below). Consistent with a solvent-exposed S4 subsite, the g4 of maltotetraose makes the least number of hydrogen bonds (four), a feature typical of a site found in group II proteins.

Extensive involvement of charged residues and syn *and* anti *stereochemistry of carboxylate sidechains*

Residues with charged sidechains make up the bulk of the hydrogen-bonding residues. Of the ten residues making hydrogen bonds with maltotetraose, seven are charged and engaged in 12 of the 15 direct hydrogen bonds with the maltotetraose. The dominant involvement of charged residues follows a similar pattern found in monosaccharide binding to ABP, GGBP and RBP [7–12] and, in general, in carbohydrate binding to other proteins [22] (unpublished data).

The *syn* configuration is the preferred and slightly more stable interaction involving carboxylate residues [25]. This agrees well with the observation that, of the eight hydrogen bonds between maltotetraose and carboxylates of Asp14, Glu44, Asp65, Glu111 and Glu153, seven are in the *syn* stereochemistry. The bond between Glu44 Oε2 and g3 OH3 is in an *anti* configuration (Figure 3b,c).

'Cooperative' hydrogen bonds

Buried sugar hydroxyl groups (those of g1, g2 and g3) are engaged in multiple hydrogen-bonding interactions with

MBP, a feature also often associated with carbohydrate binding to group I proteins [22] (unpublished data). Most of the multiple interactions are achieved by way of 'cooperative hydrogen bonds' which, as first recognized in the sugar complex of ABP [7,26], have the remarkably simple and almost general form of $(NH)_n \rightarrow OH \rightarrow O$, where OH is a sugar hydroxyl group, NH and O are protein hydrogen-bond donor and acceptor groups, respectively, and n = 1 or 2. This feature is portrayed by g1 OH1 and OH2, and g2 OH3 and OH6 of all three sugars, and g3 OH3 of maltotriose and maltotetraose. Consistent with the involvement of many charged residues in sugar-binding sites, basic and acidic sidechains provide many of the NH and O groups, respectively, that are engaged in cooperative hydrogen bonds. The exceptions in MBP are Trp62 Nε1H, Tyr155 backbone peptide NH and Tyr341 OH.

Intersugar hydrogen bonds

Excellent intersugar hydrogen-bonds (between O3 and O2′) are formed in the bound maltose and maltotriose. (The primed oxygen is contributed by the sugar unit farthest from the reducing end.) These intersugar hydrogen bonds produce a left-handed twist or curvature (about –55° between adjacent Glc units. Much longer linear maltooligosaccharides retaining these intersugar hydrogen bonds, or twist, form a left-handed helix such as that seen in amyloses. In light of the nature of the cooperative hydrogen bonds formed with O3 and O2 hydroxyls, we deduced that g1 OH3 is a donor to g2 OH2′ whereas g2 OH3 is an acceptor from g3 OH2′.

As no hydrogen bond is formed between g3 and g4, a near perfect left-handed twist for the maltotetraose is thwarted. The twist between g3 and g4 is about –75°. (A rationale for this finding is provided in the Oligosaccharide conformation section below.)

Non-involvement of glycosidic bond and ring oxygens

None of the ether oxygens of the glycosidic bonds participate in hydrogen-bonding interactions, an observation consistent with this oxygen being a poor hydrogen-bond partner. Although the ring oxygen of the reducing sugar is a somewhat better hydrogen-bond acceptor, only the ring oxygen of the reducing sugar of maltose and maltotriose is an acceptor of a hydrogen bond from a water molecule. In contrast, the ring oxygens of monosaccharides bound to ABP, GBP and RBP make hydrogen bonds with protein residues [7–12].

Comparison with MBP β-cyclodextrin binding

In spite of the fact that the three Glc residues of the bound maltotriose match those of three residues of the bound cyclodextrin [6], hydrogen-bonding interactions differ considerably between the two. The cyclodextrin makes a total of 15 hydrogen bonds, of which only four are directly formed with MBP, much less than those observed in the bound linear oligosaccharides (Table 3). The rest of the hydrogen bonds are made with water molecules. No hydrogen bond is formed with the Glc residue equivalent to g1 of the linear oligosaccharides, and only two and three hydrogen bonds are formed with the residues equivalent to g2 and g3 of the maltotriose, respectively. The hydrogen bond between g3 OH6 and Glu153 is the only bond which is identically formed with the cyclodextrin. Asp65 and Lys42 are also involved in hydrogen bonding but to different hydroxyl groups of the cyclodextrin. The observation that very few direct hydrogen bonds are formed between cyclodextrin and MBP is attributed to a wide separation between the two domains, as seen in the unbound MBP structure [6], and to a displacement of domain I, deploying most of the hydrogen-bonding residues away from their position in the bound linear oligosaccharide structures.

The bound cyclodextrin is heavily hydrated [6]: 25 ordered water molecules make 38 contacts. This degree of hydration is much greater than that seen in the bound linear oligosaccharides (Table 3) and the β-cyclodextrin dodecahydrate crystal structure [27]. This is due to the fact that four of the Glc units are exposed to the solvent and make no contact with MBP.

van der Waals interactions and aromatic residue stacking

van der Waals contacts

As expected for bound oligosaccharides which are buried and involved in extensive hydrogen-bonding interactions, features of group I proteins, a considerable number of van der Waals contacts (≤ 4.0 Å) are formed which further contribute to the stability, as well as the specificity, of the complexes. The increase of two or three hydrogen bonds in going from the bound maltose to the maltotriose or the maltotetraose (Table 3) pales in comparison with the increase in van der Waals contacts, especially in going from maltose (80 contacts) to maltotriose (107 contacts) (Table 4). Compared to the maltotriose, the binding of maltotetraose leads to an additional gain of only 11 van der Waals contacts.

The g2 residue of maltose makes the greatest number of van der Waals contacts (48). Consistent with g4 being loosely bound to a protein surface subsite (S4), it is engaged in the smallest number of van der Waals contacts. This property is characteristic of group II protein sites.

In Table 4, the van der Waals contacts are categorized into three groups: polar–polar; polar–nonpolar; and nonpolar–nonpolar. As several of the polar–polar contacts are made between the hydroxyl and ring oxygen groups of the oligosaccharides and the polar groups of MBP and water molecules, they resemble hydrogen bonds but with distances that exceeds the 3.4 Å cut-off. The same polar groups of the oligosaccharides make contacts with

Table 4

van der Waals contacts of oligosaccharides at the binding site of MBP.

	Maltose			Maltotriose				Maltotetraose				
	g1	g2	Total	g1	g2	g3	Total	g1	g2	g3	g4	Total
Polar–polar	8	5	13	8	5	7	20	7	5	7	7	26
Polar–nonpolar	21	34	55	17	24	24	65	16	24	19	12	71
Nonpolar–nonpolar	3	9	12	8	8	6	22	7	7	6	1	21
Total	32	48	80	33	37	37	107	30	36	32	20	118

nonpolar carbon atoms of the sidechains that are mostly involved in hydrogen-bonding interactions and the aromatic sidechains, resulting in polar–nonpolar contacts. In all three complexes, the number of polar–nonpolar contacts exceeds the number of polar–polar and nonpolar–nonpolar contacts.

Extensive involvement of aromatic residues

Almost all the nonpolar–nonpolar contacts are made with aromatic sidechains. Indeed, as first noted by us, the close proximity of aromatic sidechains to bound carbohydrates is a recurring feature of proteins/enzymes that bind carbohydrates [22,26]. One of the best examples of an aromatic residue–sugar interaction is found in MBP. Although this type of interaction occurs in both groups of proteins, it is generally more abundant in group I.

In particular, the stacking of the aromatic residues against sugar faces is a manifestation of the presence in sugars, especially pyranosides, of exposed clusters of nonpolar carbon atoms. In the linear α(1–4)-linked maltooligosaccharides, the CH atoms at positions 1, 2 and 4 form a nonpolar cluster on the A face of a Glc residue, whereas those at positions 3 and 5 make a cluster on the B face. The larger cluster on the A face is nearly contiguous between adjacent sugars and is confined to the outer curvature of the left-handed twist, or helix, of the maltodextrins (e.g. see Figure 5). On the other hand, the smaller cluster on the B face is confined to the inner curvature of the helix and is interrupted by the glycosidic bond oxygen. The A faces, or the outside curvature, of the oligosaccharides bound to MBP are more extensively involved in stacking interactions than the B faces, or inside curvature.

MBP is notable among the structures of proteins/enzymes that bind carbohydrates for the large abundance of aromatic residues, 16 of which are located in or near the binding site groove [4,6]. This extraordinary feature, together with the geometry of the stacking interactions, has now been further assessed using Figure 5. Five aromatic residues of MBP are intimately associated with the bound maltotriose or maltotetraose, one less than with the maltose. In contrast to the hydrogen-bonding residues, which are mostly located in domain I, more stacking aromatic residues are found in domain II (Trp230, Tyr155, Trp340 and Tyr341) than in domain I (Trp62). No aromatic residue is located close to the maltotetraose g4. The most favorable stacking interactions are demonstrated by all four aromatic residues in domain II which match the A faces or the outside curvature of the maltooligosaccharides. The oligosaccharides are cradled by the four aromatic residues originating from the wall of the domain facing the binding cleft.

The inner curvature of the three oligosaccharides is bisected by only one aromatic residue (Trp62) in domain I which plays a dual function. It makes a very minor stacking interaction with the g1 B face and donates, by way of its Nε1H, hydrogen bonds to two hydroxyls of maltose and one of maltotriose and maltotetraose (Figures 3 and 4; Table 3). A less favorable or almost complete absence of stacking interactions occurs when the polar groups of tryptophan and tyrosine make hydrogen bonds with the sugar. This is portrayed by Trp62 whose sidechain is nearly perpendicular to g2 and is located a long distance from g3 and g4 (Figures 3 and 5).

As also dramatically shown in Figure 5, Tyr341, which is found in a different conformer in the MBP–maltose and unbound structures [5], swings into the binding groove in order to participate in hydrogen-bonding and partial stacking interactions with g3 of the maltotriose and maltotetraose.

The association between aromatic residues and carbohydrates was first observed in lysozyme, the first enzyme and carbohydrate-binding protein for which a three-dimensional X-ray structure was elucidated [28–30]. The propensity of this association in many other proteins could hardly have been predicted; it is observed in all but one of over 40 different structures of protein–carbohydrate complexes [22,26] (unpublished data).

Comparison with β-cyclodextrin binding

MBP forms far fewer hydrogen bonds with β-cyclodextrin than with the linear oligosaccharides. In contrast, however, many of the interactions with the aromatic sidechains observed in the binding of linear oligosaccharides

Figure 5

Stereo view of the interactions, depicted as van der Waals dot surfaces, between aromatic residues and bound maltose (a), maltotriose (b) and maltotetraose (c). The color codes for the atoms are: C, gray; N, blue; and O, red.

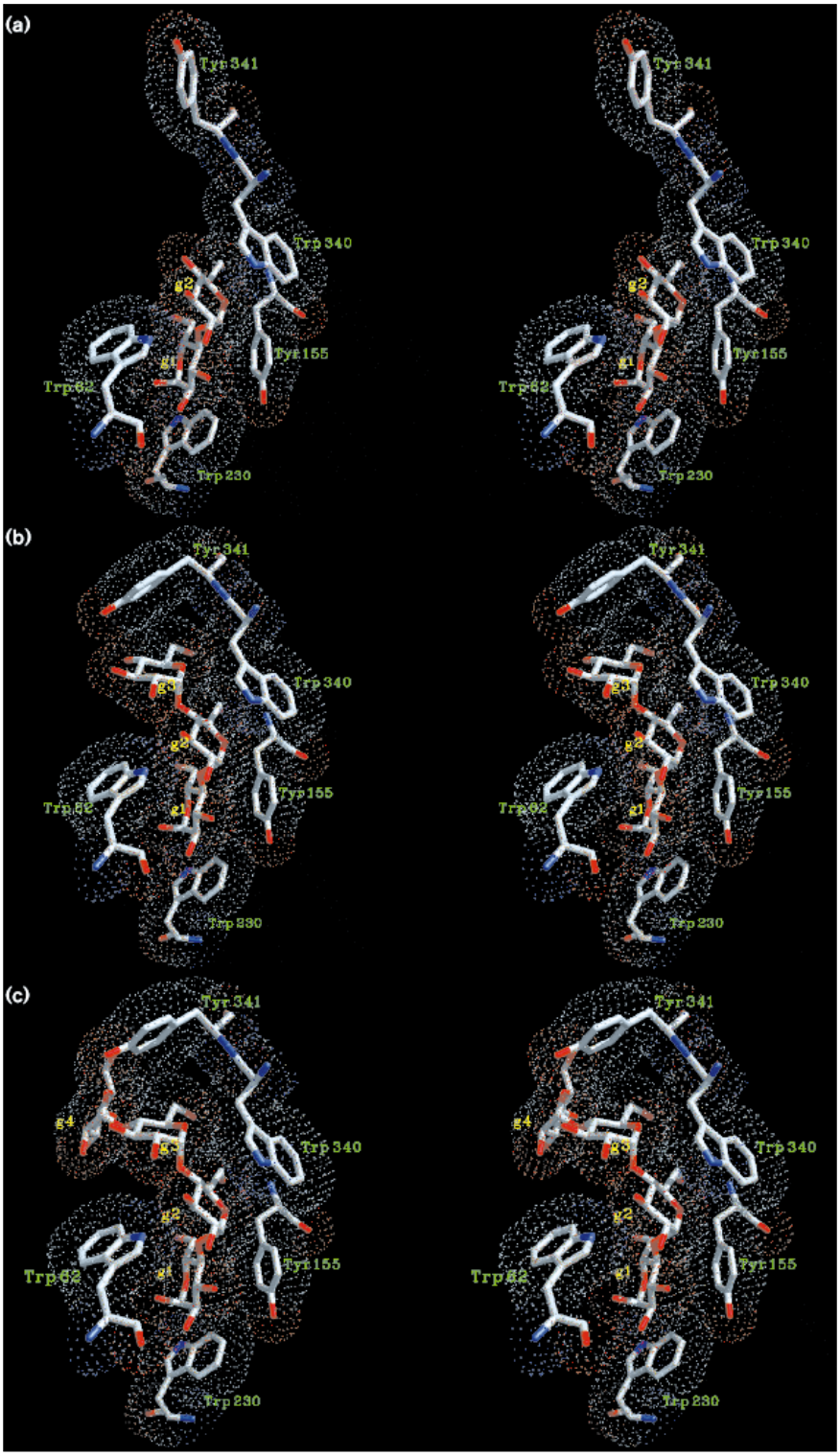

are conserved in β-cyclodextrin binding, especially those involving Trp230, Tyr155 and Trp340 of domain II [6]. This high conservation is due to a much greater similarity between the interactions of domain II, which provides most of the stacking aromatic residues, and the β-cyclodextrin or the linear oligosaccharides than between the

interactions of domain I, which deploys most of the hydrogen-bonding residues. The cyclic feature of the dextrin appears to hinder Tyr341 of domain II from making the conformational change observed in binding of the maltotriose and maltotetraose (Figure 5). This feature, combined with retention of the wide separation between the two domains seen in the unbound structure [5], also prevents Trp63 in domain I from occupying the position observed in the bound linear oligosaccharide structures (Figure 5).

Structural plasticity

Conformational changes play a key role in the ability of MBP to bind linear and cyclic oligosaccharides. Two clearly different levels of conformational changes are observed in MBP depending on the extent of these changes.

Hinge-bending between two domains

We have previously described the first level associated with the largest motion of a rigid body hinge bending between the two domains that resulted in the determination of the 'closed cleft' liganded and 'open cleft' unliganded structures [4,5]. This motion, which has been observed in several other binding proteins [18], modulates ligand access to and from the binding site groove and plays an important role in signalling in active transport and chemotaxis [5,17,18,20] (see Function section below). Moreover, as described in the preceding sections, this motion enables each domain of MBP to participate almost uniquely in carbohydrate binding — domain I in hydrogen bonding and domain II in aromatic residue interactions.

The hinge-bending motion also permits binding of the β-cyclodextrin in ways different from linear oligosaccharide binding [6]. Whereas closure of the two domains engulfs the bound linear maltodextrins (Figure 2), separation of the two domains, very similar to that observed in the ligand-free structure [5], allows the β-cyclodextrin to be wedged in the groove.

Oligosaccharide-induced conformational changes

The second major level of conformational change is confined to localized changes of residues caused by binding of linear oligosaccharides longer than maltose. These changes, most prominently displayed by Arg66 and Tyr341 (Figures 3, 4 and 5), enable the formation of nearly equivalent numbers of hydrogen bonds associated with the three oligosaccharides (Table 3). The relative change in the Arg66 conformation leads to a shift from two hydrogen bonds with maltose g2 to one hydrogen bond with the maltotriose and maltotetraose. The presence of g3 further causes Trp62 to adjust slightly, thereby abolishing one of the two hydrogen bonds between this residue and maltose g2.

The large movement of Tyr341 from its non-interacting position in the bound maltose (Figure 5a) and sugar-free structures [5] to a new position in the bound maltotriose and maltotetraose (Figures 5b,c) makes two different favorable contributions to binding. In both bound maltotriose and maltotetraose, the tyrosine aromatic sidechain partially stacks against the A face of g3, and its hydroxyl group hydrogen bonds with g3 OH3.

Specificity

Hydrogen bonds and aromatic residue stacking

From the atomic-level description of the mode of binding of the three linear oligosaccharides, it is clear that hydrogen bonds, together with the flexibility of key binding site residues, play a major role in conferring ligand specificity. The orientations of the hydrogen-bonding residues are designed for binding only maltooligosaccharides. The conformational adjustments of residues also reflect this high specificity.

Although less precise than hydrogen bonds in terms of directionality, by matching with the sugar faces aromatic residue interactions also contribute to carbohydrate recognition. Moreover, as initially enunciated, by presenting steric interference the aromatic residues disallow the binding of particular sugar epimers [7,26]. In fact, recognition of β-cyclodextrin is primarily achieved by interactions with aromatic residues, which are more abundant than direct hydrogen-bonding interactions, or by way of water molecules to MBP.

The combined arrangements of the hydrogen-bonding and aromatic stacking interactions are undoubtedly responsible for the finding that MBP does not bind lactose and other galactose-containing oligosaccharides [3].

Ordered water molecules

Before becoming recently fashionable, especially in DNA recognition, the important roles that water molecules play in ligand specificity and binding have already long been evident in protein–carbohydrate interactions [7,8,26,30–32]. The abundance of sugar hydroxyl groups makes the role of water molecules a natural feature in these interactions. An excellent example of the precise function of water molecules in conferring sugar specificity is seen in the ability of ABP to bind L-arabinose, D-galactose or D-fucose (Table 2). The high-resolution structures of the complexes of ABP with the three monosaccharides showed the interplay of two ordered water molecules and localized conformational changes in modulating the binding of each of the sugars [7,8].

Of the nine water molecules that make hydrogen bonds with the bound maltooligosaccharides (Figure 3; Table 3), only three (Wats 380, 383 and 387) do not in turn form further hydrogen bonds with protein atoms. Besides

mediating interactions between residues and sugars, water molecules modulate binding of oligosaccharides to MBP in two new ways. Firstly, a water molecule is hydrogen bonded to the hydroxyl group (OH4) of the non-reducing Glc residue destined to form a glycosidic bond in longer oligosaccharides (Figures 3 and 4). We surmise that the space occupied by the water makes way for the additional glycosidic bond. Secondly, as more water molecules are present in S1 than in the other subsites, they serve as fillers for a subsite that is larger than S2 and S3 which bind the Glc residues almost entirely by direct hydrogen bonds to MBP (Figures 3 and 4). This feature is consistent with findings that g1 can be replaced by non-sugar moieties in maltooligosaccharides with no considerable drop in affinity [33,34].

α/β Anomeric preference

Both $2F_o–F_c$ and $F_o–F_c$ electron-density maps clearly show preferential binding of only one anomer (the α form) of the three oligosaccharides (for example, see Figure 1). Similar results were also observed in the binding of monosaccharides to GGBP and RBP [9–12].

These crystallographic results appear at variance with the bimolecular reaction kinetics measured by rapid mixing stopped-flow technique, which indicated binding of both α and β anomers to MBP and GGBP [13,14]. This discrepancy has been reconciled on the basis of the infinitely faster time courses (milliseconds) in measuring ligand kinetics (Table 2) as compared with those in determining X-ray structures (several weeks or months) and of the likelihood of one anomer binding slightly tighter than the other [10]. Thus, in the case of the crystallographic analysis, the tighter complex will predominate in the long term and is eventually crystallized exclusively, as observed in MBP. NMR analysis indicated almost exclusive binding of the α anomer by MBP, which has a slightly higher affinity than the β anomer [35]. Similar explanations are applicable to the preferential binding of one anomeric form of monosaccharides bound to the GGBP and RBP in the crystal structures [10].

Kinetic data also indicated binding of both anomers of L-arabinose, D-fucose and D-glucose to ABP [14]. In this case, the data are in full agreement with the crystallographic analysis which clearly showed binding of both anomeric forms of each monopyranoside in almost equal proportions [7,8]. These results indicate identical binding affinities of both anomers.

Although the α-anomeric hydroxyl group of the oligosaccharides bound to MBP is engaged in cooperative hydrogen bonds, it makes a shorter and, thereby, stronger hydrogen bond with the Asp14 Oδ1 acceptor than with the Lys15 Nζ donor (Table 3). It has also been noted that, although the anomeric hydroxyl group of the monosaccharides bound to ABP, GGBP and RBP is engaged in multiple hydrogen bonds, the shortest hydrogen bond is formed with an aspartic acid carboxylate [10]. These observations may be related to analysis of small molecule sugar crystal structures suggesting that the anomeric hydroxyl tends to be a strong donor and a weak acceptor in hydrogen bonds [36], which is likely to be a result of the anomeric effect [37].

Binding of the β anomer of the oligosaccharides to MBP can be easily accommodated. The Asp14 anomer Oδ1, in its refined position, is also capable of accepting a hydrogen bond from the β-OH, provided that binding of the oligosaccharide β anomers will be very similar to that seen for the α-anomers. However, in this binding mode, the β-OH will be in no position to accept a hydrogen bond from Lys15, as observed with the α-OH (Figures 3 and 4; Table 3). This most likely accounts for the preferential binding of the α anomers in the crystal structures.

The ability of one aspartic acid carboxylate oxygen to hydrogen bond with both anomeric hydroxyl groups has experimental precedence. This has been clearly demonstrated in the structures of ABP with bound L-arabinose, D-galactose or D-fucose [7,8]. The carboxylate oxygen of GGBP and RBP that is seen making a strong hydrogen bond with only one anomeric hydroxyl group is, as in MBP, also in an excellent position to potentially hydrogen bond with the other anomeric hydroxyl [10].

Oligosaccharide length

Although linear maltooligosaccharides longer than maltotetraose bind to MBP and are transported [3,38], their binding affinities are not too greatly different from maltotetraose (Table 2). The increase in solvent-accessible surface at the non-reducing end of maltotetraose is a trend that should continue for longer oligosaccharides. If the first four Glc residues of longer maltodextrins bind in a similar manner to maltotetraose, then the additional Glc residues will have no subsites as well defined as S1 to S4 and, hence, will have greater exposure to the solvent than g4. This indicates that the binding site groove is designed to accommodate, with high complementarity and extensive interactions, maltodextrins no longer than a maltotetraose or possibly a maltopentaose.

In the 2.3 Å structure of the MBP–maltose complex, we observed the presence of a cluster of aromatic residues (Phe156 and Tyr210 alongside Trp230) anterior to the S1 site [4]. Although this observation suggested the possible existence of a further subsite, –S1, no study, thus far, has unambiguously shown an oligosaccharide binding mode that encompasses this presumed site. Interestingly, although S4 is devoid of aromatic residues and halfway exposed, it is this site, rather than the presumed –S1 site, which is utilized in binding of maltotetraose.

No glucose binding

Surprisingly, in spite of the presence of at least four well-defined subsites in MBP, it does not bind to glucose. The same is true for the storage site of the glycogen phosphorylase [30]. Our structural analysis indicates a rationale for this observation. As no residues or water-mediated interactions are associated with the glycosidic bond oxygens of the bound oligosaccharides, one or two hydroxyl groups of a glucose (OH4 or OH1 or both) will be left unpaired in each of the subsites. (We note that this possibility also exists in the phosphorylase–oligosaccharide complexes.) Leaving a polar group unpaired, especially in a sequestered site, is likely to be a strong factor in inhibiting glucose binding. This is clearly supported by the exquisite non-overlapping specificity of the phosphate-binding protein and the sulfate-binding protein, members of the same family of transport proteins [17,18,39,40]. Hydrogen bonds play an even more critical role in the specificity and affinity of each tetrahedral oxyanion binding protein. One unsatisfied hydrogen-bonding group amounts to a binding energy loss of about 6–7 kcal/mol [41].

Affinity

Complexes of MBP with oligosaccharides (Table 1) are among the tightest of all the proteins/enzymes binding carbohydrates. There are a number of explanations for this observation. Firstly, the oligosaccharides, with the exception of maltotetraose g4, are essentially completely buried, negating any competing, deleterious effect of the high dielectric constant bulk solvent surrounding the protein. Secondly, with the exception of exposed g4 OH4, all the hydroxyl groups of the three oligosaccharides are involved in a web of hydrogen-bonding interactions; complete pairing is important for tight binding in a buried site. Thirdly, considerable numbers of van der Waals contacts are formed. Fourthly, many of the residues making hydrogen bonds and van der Waals contacts are further held in place by networks of hydrogen bonds (data not shown). Finally, many features of the hydrogen-bonding interactions contribute to tight affinity: only a very few hydrogen bonds are long; with the exception of one hydroxyl of maltotetraose g4, all of the hydroxyl groups are involved in multiple hydrogen bonds; there is cooperativity in many of the multiple hydrogen bonds; most of the hydrogen bonds are formed with charged residues as opposed to neutral residues. Dominance of charged to neutral hydrogen bonds, combined with multiple hydrogen-bonding interactions, more than compensate for the transfer of the polar hydroxyl groups from the bulk solvent to the buried binding site; and seven of the eight hydrogen bonds with five carboxylate sidechains have the favorable *syn* configuration. Thus the combination of polar and aromatic residues are a more hospitable host for the oligosaccharide than water molecules in the unbound sugars.

The structures further shed light on why maltotriose is bound with the highest affinity (Table 2). For example, the K_d of maltotriose is 22-fold smaller than that of maltose, which is manifested as a slower off-rate for maltotriose. This is attributed, not so much as to the gain of three additional hydrogen bonds (Table 3), but to the considerable increase (40) in van der Waals interactions in binding the maltotriose over maltose. In going from bound maltotriose to maltotetraose 11 more van der Waals' contacts and no additional hydrogen bond are observed. The affinity for maltotetraose is only 11-fold less than that for maltotriose and twofold greater than for the maltose. The greater solvent exposure of g4 and, by inference, of additional Glc residues in longer oligosaccharides (see above) appears to dampen any favorable contribution of these Glc residues in the complex formation.

Oligosaccharide conformations

With retention of the $^4C_1$ pyranose ring configuration of the Glc units, the conformations of maltooligosaccharides are susceptible to change at the exocyclic torsion angle χ^5 of the primary alcohol substituents and the endocylic ϕ and ψ torsion angles of the glycosidic bonds. Including the data described here, considerable structural data on binding of α(1–4)-linked glucosyl maltodextrins to proteins are available for an unprecedented analysis of oligosaccharide conformations (Table 5). The analysis presented here includes those of maltodextrins bound to other proteins (phosphorylase storage site [30,42] and β-amylase [43]) for which coordinates are available from the Protein Data Bank and small crystal structures of α-maltose [44], methyl-β-maltotrioside [45] and β-cyclodextrin dodecahydrate [27].

Primary alcohol (χ^5)

Of the three torsion angles, the exocyclic angle χ^5, defined as the angle of the atoms C4–C5–C6–O6 is subject to the least constraints, allowing free rotation of OH6 about C5–C6. Nevertheless, it is surprising to find that the χ^5 angle of the Glc residues of all three oligosaccharides bound to MBP is similar; they all exhibit a *trans* conformation, including the primary alcohol of g4 which does not make contact with the protein. This conformation is also shown by the two primary alcohols of the α-maltose crystal structure. Whereas this conformation is exhibited by all but one of the primary alcohols of the bound β-cyclodextrin, it is manifested in only three of the β-cyclodextrin dodecahydrate crystal structure. This conformation is exhibited by only one of the 5 ordered Glc units (g4) of the maltoheptaose bound to phosphorylase and one of the maltotetraose (g1) bound to β-amylase. All the primary alcohol substituents listed in Table 5 that do not have *trans* configuration, including all those of the methyl-β-maltotrioside, have +*gauche* conformation. The orientation of the O6 hydroxyl is selected by the environment of the sugar and its interaction with the protein, or its interaction

Table 5

Sugar conformation of maltooligosaccharides.

Protein	Oligosaccharide	Glycosidic bond (°)*		O2′–O3 Hydrogen bond (Å)†	χ^5		Reference
		ϕ	ψ		Glc unit	Value (°)*	
MBP	Maltose						This paper
	g2-g1	107	–138	2.8	g1	–170	
					g2	–167	
MBP	Maltotriose						This paper
	g2-g1	100	–137	2.7	g1	–165	
	g3-g2	103	–124	2.8	g2	–165	
					g3	–172	
MBP	Maltotetraose						This paper
	g2-g1	110	–135	2.7	g1	–169	
	g3-g2	106	–124	2.6	g2	–170	
	g4-g3	80	–151	(4.0)	g3	–156	
					g4	178	
MBP	β-Cyclodextrin						[6]
	g2-g1	106	–107	3.0	g1	–175	
	g3-g2	103	–124	2.9	g2	–148	
	g4-g3	140	–101	3.0	g3	–165	
	g5-g4	96	–114	3.2	g4	175	
	g6-g5	110	–106	2.7	g5	–165	
	g7-g6	112	–136	2.6	g6	108	
	g8-g1	122	–112	2.7	g7	–136	
Phosphorylase	Maltoheptaose						[42]
	g4-g3	117	153	3.4	g3	35	
	g5-g4	92	–161	(3.5)	g3	171	
	g6-g5	95	–129	3.3	g4	66	
	g7-g6	111	–137	2.6	g5	47	
					g6	61	
β-Amylase	Maltotetraose‡						[43]
	g2-g1	111	–113	2.8	g1	–160	
	g3-g2	153	100	(5.5)	g2	64	
	g4-g3	66	–151	(4.4)	g3	65	
					g4	61	
	α-Maltose						[44]
	g2-g1	116.1	–117.9	2.77	g1	175.5	
					g2	171.3	
	Methyl-β-maltotrioside						[45]
	g2-g1	82.8	–151.8	(3.87)	g1	67.0	
	g3-g2	82.3	–148.9	(3.63)	g2	57.9	
					g3	62.3	
	β-Cyclodextrin dodecahydrate						[27]
	g2-g1	107.7	–109.4	2.90	g1	58.7	
	g3-g2	110.8	–114.1	2.78	g2	60.0	
	g4-g3	120.1	–109.7	2.77	g3	50.8	
	g5-g4	103.0	–125.7	2.86	g4	–175.4	
	g6-g5	119.2	–95.8	2.86	g5	52.2	
	g7-g6	110.5	–106.6	2.96	g6	–169.4	
	g1-g7	102.6	–121.2	2.86	g7	–174.0	

The data were either obtained from the refined structures reported here, from the Protein Data Bank, or from the Cambridge Data Bank for small molecule structures. *The endocyclic ϕ and ψ torsion angles about the glycosidic bond for linear oligosaccharides are defined by O5′–C1′–O4–C4 and C1′–O4–C4–C5, respectively, where the primed atoms are contributed by the sugar residue farthest from the reducing end. For the cyclodextrins, the Glc unit identifications were based on the overlap between the bound cyclodextrin and maltotriose [6]. The exocyclic angle χ^5 of the alcohol groups is defined as the torsion angle of the atoms C4–C5–C6–O6. †Hydrogen bonds between Glc units, where the primed atoms are defined as in the preceding footnote. The values in parentheses exceed the maximum hydrogen bond distance of 3.4 Å. ‡In order to be consistent with the other entries in the table, the identifications of the Glc units are in the reverse order as described in the paper by Mikami *et al*. [43] and in the coordinates deposited in the PDB (ID code 1BYB).

in the crystal lattice for the small molecule structures, as opposed to energy considerations arising from the sugar structure itself.

Glycosidic bond

The endocyclic ϕ and ψ torsion angles about the glycosidic bond are defined by O5′–C1′–O4–C4 and C1′–O4–C4–C5, respectively, where the primed atoms are contributed by the sugar residue farthest from the reducing end. The three sets of torsion angles of the maltotetraose bound to MBP fall into two distinct ranges. The first and second sets relating g2 to g1 and g3 to g2, respectively, are similar. They permit the formation of the intersugar hydrogen bond between O2′ and O3. The only other occurrence of these angles is in the glycosidic bonds g6–g5 and g7–g6 in oligosaccharide bound to phosphorylase. These angles are not the same as those found in the α-maltose small molecule crystal structure, which also permit formation of the intersugar hydrogen bond. The angles in the α-maltose crystal structure are also exhibited by the first glycosidic bond of the maltotetraose bound to β-amylase and by almost all of the bonds in the bound and free β-cyclodextrin.

The third set of glycosidic angles of the MBP-bound maltotetraose are significantly different from the first two. This second conformation prevents formation of the hydrogen bond between the Glc residues and is also seen in the identical glycosidic bond of the maltotetraose bound to amylase and in both bonds of methylmaltotrioside. Another possible occurrence of this set of torsion angles in a linear maltodextrin is in the complex of phosphorylase with maltoheptaose (between g5–g4). This conformation may also be exhibited by the glycosidic bond between g3 and g2 of the linear maltohexaose bound to the maltoporin [24].

This second glycosidic bond conformation in the protein-bound oligosaccharides appears to be a local minimum conformation for linear maltodextrins, which occurs in the presence of external hydrogen-bonding opportunities with residues and disallows the intersugar hydrogen bond. It is an acidic residue that contributes primarily to the stability of this glycosidic conformation in MBP (Glu44 as shown in Figures 3 and 4), phosphorylase (Glu433) [30,42] and β-amylase (Asp101) [43].

In the maltotetraose bound to MBP and β-amylase, the Glc residue which is not involved in the intersugar hydrogen bond is preceded by three Glc residues. On the other hand, the equivalent Glc in the maltoheptaose bound in the glycogen phosphorylase storage site is preceded by four Glc residues. Thus, we cannot conclude that the sequence of torsion angles is constant, or that we have discovered a maltodextrin conformation that is likely to be stable in solution. Instead, we have identified two local minima for the maltodextrin population, both convenient for binding by protein molecules, or stabilized by complex formation. For purposes of protein engineering and drug design, this is perhaps a more useful result.

The variability of the glycosidic bonds is further demonstrated in the maltotetraose bound to the β-amylase which displays yet a third different glycosidic bond conformation between g3–g2. This conformation is not observed in the structures of any other maltooligosaccharides, bound or unbound to other proteins. This conformation also disallows formation of the intersugar hydrogen bond.

As only three carefully studied cases have been sampled here, caution must be made in making generalizations about bound maltooligosaccharide conformations. However, the binding sites are sufficiently different within the limitations of their function that this is at least not a biased sample. The glycogen storage site of the phosphorylase is typical of carbohydrate-binding group II proteins whereas the MBP site is more closely aligned with group I. Although the site in the β-amylase is near the surface, it is partly buried. The glycogen storage and β-amylase sites have a lower affinity (millimolar range) for maltooligosaccharides than does MBP. Five aromatic sidechains surround the maltotetraose bound to MBP, whereas only one is present in the maltoheptaose-bound storage site of phosphorylase. At least four aromatic residues are close to the maltotetraose bound to the β-amylase.

MBP and maltoporin structures

Maltoporin and MBP are functionally linked. Maltoporin provides a specific passage for maltooligosaccharides across the outer membrane of *Escherichia coli* and *Salmonella typhimurium* which are then taken up by MBP. The structures of maltoporin complexed with maltooligosaccharides have been determined, albeit at much lower resolutions (2.6 to 3.2 Å) [24] than those of MBP. Nevertheless, a qualitative comparison of several features of oligosaccharide binding to MBP with those of maltoporin is illuminating. As the oligosaccharide-binding site of maltoporin is located within a channel, the site technically belongs to group I. However, there are some features of this site more characteristic of group II proteins. Several of the Glc residues of maltohexaose bound to maltoporin have B factors significantly higher than the mean value of the protein structure. Indeed, well-defined density is seen for only three Glc residues (g2 to g4). Moreover, the K_d values of maltoporin–maltooligosaccharide complexes are in the low millimolar range [46].

Nevertheless, MBP and maltoporin share, to varying degrees, several prominent features of oligosaccharide binding. In the maltoporin-bound maltohexaose, the three ordered Glc units make ten direct hydrogen bonds, four less than formed in the MBP–maltotriose complex (Table 3).

Maltoporin also makes extensive use of charged residues in hydrogen bonding oligosaccharides: six of the seven residues involved in the hydrogen bonds are charged. Two of the hydroxyl groups belonging to g3 and g4 of the maltohexaose are also involved in cooperative hydrogen bonds, however, this is considerably less than the number seen in the MBP–maltotriose complex.

The involvement of several aromatic residues in oligosaccharide binding is where MBP and maltoporin share the greatest similarity. There are six aromatic residues close to the oligosaccharides bound to maltoporin, three of which (Tyr41, Tyr6 and Trp420) stack against the A faces of the outer curvature of the three ordered Glc units. This stacking interaction is very similar to that of the three aromatic residues of MBP with the identical faces of maltotriose (Figure 5b). Tyr118 of maltoporin is in a location similar to that of Trp62 of MBP, which interacts with atoms in the inner curvature (B faces) of the bound oligosaccharide (Figure 5b).

Function

The X-ray crystallographic analysis of at least a dozen binding protein receptors exhibiting a wide variety of specificity (carbohydrates, amino acids, oligopeptides, oxyanions and polyamine), has uniquely contributed to our understanding, at the atomic level, of the structure and function of this family of proteins [17,18,20]. This analysis revealed similar structures despite the fact that these proteins have little in common with respect to size (26–58 kDa), amino acid content and sequence, and ligand specificity. The finding that the two domains of the binding proteins exhibit the 'Rossmann fold' (or 'mononucleotide-binding motif') provided one of the first pieces of evidence demonstrating the existence of this fold in totally unrelated proteins.

The dominance of hydrogen bonds in ligand binding seen in all binding proteins [17,18] is further solidified by the structures reported here. As hydrogen bonds are highly directional, they play a major role in conferring specificity. Moreover, a feature crucial to active transport is that hydrogen bonds are stable enough to provide the requisite ligand-binding affinities but are of sufficiently low strength to allow rapid ligand dissociation. Even in cases where salt links are formed in complex formation, the affinities of these complexes do not differ much from those without salt links [20,47].

The present study has important new bearings on the function of MBP. The study has shown how MBP is able to recognize and bind tightly three linear maltooligosaccharides, a prerequisite for active transport, and has also indicated how MBP can bind both anomeric forms of the oligosaccharides, an additional non-discriminatory feature advantageous to the bacteria.

Of critical functional importance is the finding that the three bound structures are essentially identical (Figure 2), with the relative orientation of the two domains remaining the same. This closed, ligand-bound structure ensures productive interaction with the cytoplasmic membrane protein components which carry out actual ligand translocation. The ligand-bound closed MBP structure is presumably recognized by the membrane components in preference to the open unliganded structure, thereby triggering active transport or chemotaxis [4,5,7,9]. The tertiary structures of MBP, along with the knowledge of sites of mutations that affect transport or chemotaxis but not sugar binding (reviewed in [48]), showed that the two domains are utilized in the productive association with the membrane components of transport or chemotaxis [4,5], a feature suggested by the first structure determination of a periplasmic binding protein [49]. An open structure like that of the sugar-free protein [5] prevents productive interaction between the binding protein and membrane components.

Although oligosaccharides composed of two to seven Glc units are bound by MBP and transported, recognition and binding affinity are almost entirely provided by the first four Glc units from the reducing end. Interestingly, although g4 of maltotetraose (and by inference the Glc units of longer oligosaccharides) is exposed on the surface of MBP, this sugar unit does not appear to interfere with the productive interaction between the receptor and membrane components.

The involvement of the g1 OH6 in hydrogen bonding with water molecules exclusively makes it a promising site for initial recognition/interaction of the oligosaccharide with the membrane bound transport components (MalFG) of the maltooligosaccharide system. As the hydroxyl is already exposed, the ease of forming an interaction with the MalFG complex is enhanced. There is also already indication that it is this hydroxyl group which is recognized by the MalFG membrane complex from inhibition studies involving maltodextrin analogs [33].

Biological implications

Active-transport processes perform a vital function in the life of a cell by maintaining a relative constancy of the intracellular milieu and regulating the entrance and exit of the various substances necessary for metabolic activity. Maltodextrins/maltooligosaccharides represent a commonly available source of energy. The high affinity transport of these oligosaccharides by the maltodextrin-binding protein (MBP)-dependent active-transport system (or permease) provides bacteria with a source of these important nutrients. The active-transport system comprises an initial high-affinity extracytoplasmic receptor (MBP), which binds oligosaccharides with two to seven α(1–4)-linked glucosyl units, and a set of cytoplasmic

membrane-associated proteins. MBP also plays a role in chemotaxis, an important process for the survival (and control) of microorganisms.

The determination of the high-resolution structures (1.67 to 1.8 Å) of complexes of MBP with maltose, maltotriose, and maltotetraose (K_ds of 35, 1.6 and 23 μM, respectively) provide extensive atomic-level details of oligosaccharide recognition and binding. The structure of MBP is composed of two globular domains separated by a ligand-binding site groove which can accommodate four glucosyl units. Whereas the maltose, maltotriose and the first three glucose units of the maltotetraose are essentially buried in the groove between the two domains, the fourth, non-reducing glucosyl unit of maltotetraose is half exposed to the bulk solvent. Hinge-bending between the two domains allows the participation of both domains in binding and sequestering the ligands. The structure of MBP has been observed in two forms: the 'closed' linear oligosaccharide-bound forms seen here, and the 'open' unbound form. The closed structure is presumably recognized by the membrane components of the active-transport system, in preference to the open form, and therefore initiates active transport. The observation that the three bound structures are essentially identical ensures productive interaction with the membrane protein components which are distinct for transport and chemotaxis.

Materials and methods

Materials

The very highest purity maltose, maltotriose and maltotetraose were obtained from Pfanstiehl Laboratories. Polyethylene glycol (PEG) 6000 was obtained from Fluka AG. All other reagents and chemicals were of analytical reagent grade.

Protein purification and crystallization

The methods used in the purification and structure determination of MBP have been extensively described [6]. Briefly, MBP was purified from *Escherichia coli* LA3400, dialyzed against the buffer solution of 0.02% sodium azide, 10 mM 2[*N*-morpholino]ethanesulfonic acid (MES), pH 6.2, and then concentrated to approximately 25 mg/ml. Crystals of MBP with bound oligosaccharides were obtained via the hanging-drop method. Crystals were grown in 25 μl drops of MBP (3.5 mg/ml), 1 mM of each maltodextrin, 16% (w/v) PEG 6000 in the buffer solution suspended over 1 ml 22% PEG at 4°C. Crystals were harvested into a stabilizing solution of 1 mM maltodextrin with 25% PEG 8000 in the buffer solution. Crystals (C2 space group) of the three complexes are isomorphous with unit cell dimensions of a = 105.88 Å, b = 68.61 Å, c = 57.94 Å, and β = 112.54° with maltose, a = 106.07 Å, b = 68.44 Å, c = 57.93 Å, and β = 112.51° with maltotriose and a = 106.67 Å, b = 68.38 Å, c = 58.44 Å, and β = 112.00° with maltotetraose.

Structure determination and refinement

Diffraction intensities were measured from one crystal for each complex using a dual detector SDMS system mounted on a Rigaku RU200 rotating anode (Cu Kα target) equipped with a graphite crystal monochromator and operated at 90 ma and 50 kv. The percentage of completeness with 2σ cut-off was 90% for the MBP–maltose data to 1.67 Å resolution, 86% for the MBP–maltotriose 1.7 Å data, and 84% for the MBP–maltotetraose 1.8 Å data (Table 1).

The structures of the MBP–maltotriose and MBP–maltotetraose complexes were determined by direct phasing with the PROLSQ [50] refined 1.7 Å structure of the MBP–maltose [16] with the bound maltose and ordered water molecules coordinates deleted. The model of the maltotriose or maltotetraose was fitted straightforwardly to the density, which was well defined, in the latter stages of structure refinement. Restrained least squares refinement was done with PROLSQ [50] following the strategy briefly described for the MBP–maltose complex structure [16]. All density fitting and examination of models was done with CHAIN [51].

Accession numbers

The three sets of coordinates have been deposited in the Protein Data Bank with accession codes 1ANF, 3MBP and 4MBP for the MBP–maltose, MBP–maltotriose and MBP–maltotetraose complexes, respectively.

Acknowledgements

This work was supported in part by grants from the NIH and the Welch Foundation. We thank the assistance of William Meador and Timothy Reynolds. FAQ is a Howard Hughes Medical Institute Investigator.

References

1. Boos, W. & Lucht, J.M. (1996). Periplasmic binding protein-dependent ABC transporters. In *Escherichia coli and Salmonella Cellular and Molecular Biology.* (Neidhardt, F.C., ed.), pp. 1175–1209, ASM Press, Washington, DC.
2. Stock, J.B. & Surette, M.G. (1996). Chemotaxis. In *Escherichia coli and Salmonella Cellular and Molecular Biology.* (Neidhardt, F.C., ed.), pp. 1103–1129, ASM Press, Washington, DC.
3. Kellerman, O. & Szmelcman, S. (1974). Active transport of maltose in *Escherichia coli* K-12. Involvement of a periplasmic maltose-binding protein. *Eur. J. Biochem.* 47, 139–149.
4. Spurlino, J.C., Lu, G.-Y. & Quiocho, F.A. (1991). The 2.3 Å resolution structure of the maltose- or maltodextrin-binding protein, a primary receptor of bacterial active transport and chemotaxis. *J. Biol. Chem.* 266, 5202–5219.
5. Sharff, A.J., Rodseth, L.E., Spurlino, J.C. & Quiocho, F.A. (1992). Crystallographic evidence of a large ligand-induced hinge-twist motion between the two domains of the maltodextrin-binding protein involved in active transport and chemotaxis. *Biochemistry* 31, 10657–10663.
6. Sharff, A.J., Rodseth, L.E. & Quiocho, F.A. (1993). Refined 1.8 Å structure reveals the mode of binding of β-cyclodextrin to the maltodextrin binding protein. *Biochemistry* 32, 10553–10559.
7. Quiocho, F.A. & Vyas, N.K. (1984). Novel stereospecificity of the L-arabinose-binding protein. *Nature* 310, 381–386.
8. Quiocho, F.A., Wilson, D.K. & Vyas, N.K. (1989). Substrate specificity and affinity of a protein modulated by bound water molecules. *Nature* 340, 404–407.
9. Vyas, N.K., Vyas, M.N. & Quiocho, F.A. (1988). Sugar- and signal-transducer binding sites of the *Escherichia coli* galactose chemoreceptor protein. *Science* 242, 1290–1295.
10. Vyas, M.N., Vyas, N.K. & Quiocho, F.A. (1994). Crystallographic analysis of the epimeric, and anomeric specificity of the periplasmic transport/chemosensory protein receptor for D-glucose, and D-galactose. *Biochemistry* 33, 4762–4768.
11. Zou, J., Flocco, M.M. & Mowbray, S.L. (1993). The 1.7 Å refined X-ray structure of the periplasmic glucose/galactose receptor from *Salmonella typhimurium. J. Mol. Biol.* 233, 7399–752.
12. Mowbray, S.L. & Cole, L.B. (1992). 1.7 Å X-ray structure of the periplasmic ribose receptor from *Escherichia coli. J. Mol. Biol.* 225, 155–175.
13. Miller, D.M., Olson, J.S. & Quiocho, F.A. (1980). The mechanism of sugar binding to the periplasmic receptor for galactose chemotaxis and transport in *Escherichia coli. J. Biol. Chem.* 255, 2465–2471.
14. Miller, D.M., Olson, J.S., Pflugrath, J.W. & Quiocho, F.A. (1983). Rates of ligand binding to periplasmic binding proteins involved in bacterial transport and chemotaxis. *J. Biol. Chem.* 258, 13193–13198.
15. Ferenci, T. & Boos, W. (1980). The role of the *Escherichia coli* λ receptor in the transport of maltose and maltodextrins. *J. Supramol. Struct.* 94, 101–116.
16. Spurlino, J.C., Rodseth, L.E. & Quiocho, F.A. (1992). Atomic interactions in protein-carbohydrate complexes: tryptophan residues in the periplasmic maltodextrin receptor for transport and chemotaxis. *J. Mol. Biol.* 226, 15–22.

17. Quiocho, F.A. (1991). Atomic structures and function of periplasmic receptors for active transport and chemotaxis. *Curr. Opin. Struct. Biol.* **1**, 922–933.
18. Quiocho, F.A. & Ledvina, P.S. (1996). Atomic structure and specificity of bacterial periplasmic receptors for active transport and chemotaxis: variation of common themes. *Mol. Microbiol.* **20**, 17–25.
19. Sugiyama, S., *et al.*, & Morikawa, K. (1996). The 1.8-Å X-ray structure of the *Escherichia coli* PotD protein complexed with spermidine and the mechanism of polyamine binding. *Protein Sci.* **5**, 1984–1990.
20. Yao, N., Trakhanov, S. & Quiocho, F.A. (1994). Refined 1.89 Å structure of the histidine-binding protein complexed with histidine, and its relationship with other active transport/chemosensory proteins. *Biochemistry* **33**, 4769–4779.
21. Quiocho, F.A., Vyas, N.K. & Spurlino, J.C. (1989). Atomic interactions between proteins and carbohydrates. *Trans. Am. Cryst. Assoc.* **25**, 23–35.
22. Vyas, N.K. (1991). Atomic features of protein–carbohydrate interactions. *Curr. Opin. Struct. Biol.* **1**, 732–740.
23. Divne, C., *et al.*, & Jones, A. (1994). The three-dimensional structure of the catalytic core of cellobiohydrolase I from *Trichoderma reesei*. *Science* **265**, 524–528.
24. Dutzler, R., Wang, Y.-F., Rizkallah, P.J., Rosenbusch, J.P. & Schirmer, T. (1996). Crystal structure of various maltooligosaccharides bound to maltoporin reveal a specific sugar translocation pathway. *Structure* **4**, 127–134.
25. Gandour, R.D. (1981). On the importance of orientation in general base catalysis by carboxylate. *Bioorg. Chem.* **10**, 169–176.
26. Quiocho, F.A. (1986). Carbohydrate-binding proteins: tertiary structures and protein–sugar interactions. *Annu. Rev. Biochem.* **55**, 287–315.
27. Lindner, K. & Saenger, W. (1982). Crystal and molecular structure of cyclohepta-amylose dodecahydrate. *Carbohydr. Res.* **99**, 103–115.
28. Blake, C.C.F., Koening, D.F., Mair, G.A., North A.C.T., Phillips, D.C. & Sarma, V.R. (1965). Structure of hen egg white lysozyme. A three-dimensional Fourier synthesis at 2.0 Å resolution. *Nature* **206**, 757–761.
29. Johnson, L.N. & Phillips, D.C. (1965). Structure of some crystalline lysozyme–inhibitor complexes determined by X-ray analysis at 5 Å resolution. *Nature* **206**, 761–763.
30. Johnson, L.N., Cheetham, P.J., McLaughlin, P.J., Acharya, K.R., Barford, D. & Phillips, D.C. (1988). Protein–oligosaccharide interactions: lysozyme, phosphorylase, amylases. *Curr. Top. Microbiol. Immunol.* **139**, 81–134.
31. Blake, C.C.F., Johnson, L.N., Mair, G.A., North, A.C.T., Phillips, D.C. & Sarma, V.R. (1967). Crystallographic studies of the activity of hen egg-white lysozyme. *Proc. R. Soc. Lond. [Biol] B* **167**, 378–388.
32. Quiocho, F.A. (1988). Molecular features and basic understanding of protein–carbohydrate interactions: the arabinose-binding protein–sugar complex. *Curr. Top. Microbiol. Immunol.* **139**, 135–148.
33. Ferenci, T., Muir, M., Lee, K.-S. & Maris, D. (1986). Substrate specificity of the *Escherichia coli* maltodextrin transport system and its component proteins. *Biochim. Biophys. Acta* **860**, 44–50.
34. Thieme, R., Lay, H., Oser, A., Lehmann, J., Wrissenberg, S. & Boos, W. (1986). 3-Azi-1-methoxybutyl D-maltooligosaccharides specifically bind to the maltose/maltooligosaccharide-binding protein of *Escherichia coli* and can be used as photoaffinity labels. *Eur. J. Biochem.* **160**, 83–91.
35. Gehring, K., Williams, P.G., Pelton, J.G., Morimoto, H. & Wemmer, D.E. (1991). Tritium NMR spectroscopy of ligand binding to maltose-binding protein. *Biochemistry* **30**, 5524–5531.
36. Jeffrey, G.A. (1990). Crystallographic studies of carbohydrates. *Acta Cryst. B* **46**, 89–103.
37. Lemieux, R.U. (1963). Rearrangements and isomerizations in carbohydrate chemistry. In *Molecular Rearrangements.* (deMayo, ed.), pp. 713–769, Wiley-Interscience, New York, NY.
38. Ferenci, T. (1980). The recognition of maltodextrins by *Escherichia coli*. *Eur. J. Biochem.* **108**, 631–636.
39. Pflugrath, J.W. & Quiocho, F.A. (1985). Sulphate sequestered in the sulphate-binding protein of *Salmonella typhimurium* is bound solely by hydrogen bonds. *Nature* **314**, 257–260.
40. Luecke, H. & Quiocho, F.A. (1990). High specificity of a phosphate transport protein determined by hydrogen bonds. *Nature* **347**, 402–406.
41. Jacobson, B.L. & Quiocho, F.A. (1988). Sulfate-binding protein dislikes protonated oxyacids: a molecular explanation. *J. Mol. Biol.* **204**, 783–787.
42. Johnson, L.N., Acharya, K.R., Joran, M.D. & McLaughlin, P.J. (1990). Refined crystal structure of the phosphorylase-heptulose 2-phosphate-oligosaccharide–AMP complex. *J. Mol. Biol.* **211**, 645–661.
43. Mikami, B., Degano, M., Hehre, E.J. & Sacchettini, J.C. (1993). Crystal structures of soybean β-amylase reacted with β-maltose and maltal: active site components and their apparent role in catalysis. *Biochemistry* **33**, 7779–7787.
44. Takusagawa, F. & Jacobson, R.A. (1978). The crystal and molecular structure of α-maltose. *Acta. Cryst. B* **34**, 213–218.
45. Pangborn, W., Langs, D. & Perez, S. (1985). Regular left-handed fragment of amylose: crystal and molecular structure of methyl-α-maltotrioside. *Int. J. Biol. Macromol.* **7**, 363–369.
46. Schülein, K. & Benz, R. (1990). LamB (maltoporin) of *Salmonella typhimurium*: isolation, purification a comparison of sugar binding with LamB of *Escherichia coli*. *Mol. Microbiol.* **4**, 625–362.
47. Yao, N., Ledvina, P.S., Choudhary, A. & Quiocho, F.A. (1996). Modulation of a salt link does not affect binding of phosphate to its specific active transport receptor. *Biochemistry* **35**, 2079–2085.
48. Martineau, P., Szmelcman, S., Hofnung, M., Spurlino, J.C. & Quiocho, F.A. (1990). Progress in the identification of interaction sites on the periplasmic maltose binding protein from *E. coli*. *Biochimie* **72**, 397–402.
49. Quiocho, F.A., Gilliland, G.L. & Phillips, G.N., Jr. (1977). The 2.8-Å resolution structure of the L-arabinose-binding protein from *Escherichia coli*. *J. Biol. Chem.* **252**, 5142–5149.
50. Hendrickson, W.A. (1985). Stereochemically restrained refinement of macromolecular structures. *Methods Enzymol.* **115**, 252–270.
51. Sack, J.S. (1988). CHAIN – a crystallographic modeling program. *J. Mol. Graph.* **6**, 244–245.